AD_____
(Leave blank)

Award Number:
W81XWH-06-1-0378

TITLE:
The role of interleukin-6/GP130 signaling in prostate cancer progression and its contribution to bone metastasis morbidity

PRINCIPAL INVESTIGATOR:
Richard P. Redvers, Ph.D.

CONTRACTING ORGANIZATION:
Monash Institute of Medical Research
Clayton, Victoria 3168 AUSTRALIA

REPORT DATE:
November 2008

TYPE OF REPORT:
Final

PREPARED FOR: U.S. Army Medical Research and Materiel Command
Fort Detrick, Maryland 21702-5012

DISTRIBUTION STATEMENT: (Check one)

X Approved for public release; distribution unlimited

☐ Distribution limited to U.S. Government agencies only; report contains proprietary information

REPORT DOCUMENTATION PAGE

Form Approved
OMB No. 0704-0188

1. REPORT DATE *(DD-MM-YYYY)*	**2. REPORT TYPE**	**3. DATES COVERED** *(From - To)*
15-11-2008	Final	1 MAR 2006 - 15 OCT 2008

4. TITLE AND SUBTITLE
The role of interleukin-6/GP130 signaling in prostate cancer progression and its contribution to bone metastasis morbidity

5a. CONTRACT NUMBER
W81XWH-06-1-0378

5b. GRANT NUMBER

5c. PROGRAM ELEMENT NUMBER

6. AUTHOR(S)
Richard Paul Redvers

5d. PROJECT NUMBER

5e. TASK NUMBER

5f. WORK UNIT NUMBER

7. PERFORMING ORGANIZATION NAME(S) AND ADDRESS(ES)
Monash Institute of Medical Research
Monash Medical Centre
246 Clayton Rd
Clayton, Victoria 3168
Australia

8. PERFORMING ORGANIZATION REPORT NUMBER

9. SPONSORING / MONITORING AGENCY NAME(S) AND ADDRESS(ES)
U.S. Army Medical Research And Materiel Command
Fort Detrick, Maryland 21702-5012

10. SPONSOR/MONITOR'S ACRONYM(S)

11. SPONSOR/MONITOR'S REPORT NUMBER(S)

12. DISTRIBUTION / AVAILABILITY STATEMENT
Approved for public release; distribution unlimited

13. SUPPLEMENTARY NOTES

14. ABSTRACT
The cytokine interleukin-6 (IL-6) is strongly implicated in primary prostate cancer (PrCa) growth and the progression to bone metastasis. While expression and localization of IL-6 and its receptors gp130 and IL-6R have been studied in organ-confined PrCa, these key mediators of the IL-6/gp130 signaling pathway have not been previously assessed in prostatic bone metastases. Our investigations with archival patient biopsies revealed that all PrCa bone metastases examined (n=14) expressed IL-6 on an overwhelming majority of cells (78±5%). The IL-6 receptor (IL-6R) was expressed in 11/14 cases in 77±7% of PrCa cells. Activated (phosphorylated) gp130 was expressed in all but one case (13/14), and was expressed in the majority of cells (79±5%) in 9/14 cases. Importantly, when IL-6R was localized to cell membranes (4/11 cases), phospho-gp130 and IL-6 were also detected at the cell membrane. Thus, members of the IL-6/gp130 axis are present in a high proportion of bone metastatic PrCa cells in most cases. The importance of this pathway was further elucidated by characterizing anti-IL-6-treated BM18 transplants. Understanding the role of IL-6/gp130 signaling in this disease may lead to identification of novel targets and therapeutic strategies to improve and extend the quality of life for PrCa patients.

15. SUBJECT TERMS
prostate cancer, interleukin-6, gp130, androgen-dependent, androgen-withdrawal, xenograft, osteosclerotic, osteoblastic, bone metastasis, apoptosis

16. SECURITY CLASSIFICATION OF:			**17. LIMITATION OF ABSTRACT**	**18. NUMBER OF PAGES**	**19a. NAME OF RESPONSIBLE PERSON**
a. REPORT	**b. ABSTRACT**	**c. THIS PAGE**			USAMRMC
U	U	U	UU	28	**19b. TELEPHONE NUMBER** *(include area code)*

Table of Contents

Introduction

Prostate cancer (PrCa) is the leading cause of male cancer death in Western civilization. Interleukin-6 (IL-6) is a cytokine implicated in primary PrCa growth and survival post-androgen withdrawal. Moreover, IL-6 is strongly associated with bone metastasis, a major cause of morbidity in PrCa patients. This project aims to investigate the IL-6 axis in a novel *in vivo* PrCa xenograft model (BM18) of androgen-dependent growth (McCulloch et al., 2005) and osteosclerotic bone metastasis. The IL-6/gp130 signaling pathway was also investigated using PrCa bone metastases from human patient biopsies. Pursuit of the aims outlined herein will greatly improve our understanding of the role of IL-6/gp130 signaling in prostate cancer growth, regression, survival post-androgen withdrawal and bone metastasis. This study provides a unique opportunity to examine the role of IL-6/gp130 signaling in a model that closely mimics human PrCa growth, progression and regression as well as osteosclerotic bone remodeling. Disease recurrence and osteosclerotic metastases are poorly understood processes that cause immense suffering, culminating in a painful demise. Understanding the role of IL-6/gp130 signaling molecules in this disease may lead to identification of novel targets and therapeutic strategies to improve and extend the quality of life for PrCa patients.

Body

Aim 1. Characterize the role of IL-6 in prostate cancer cell survival, post-androgen withdrawal

Task 1. To obtain BM18 tumor tissue that has regressed post-androgen withdrawal +/- IL-6 neutralization, or IL-6 neutralization alone, at time-points <1 week before the tumor regresses to non-detectable.

Anesthetized male SCID mice were implanted subcutaneously with a ~1mm^3 piece of BM18 tumor in the following groups*:

Table I BM18 recipient groups selected for treatment

	4 weeks	8 weeks	12 weeks
Untreated	6	6	6
Castrated	6	6	6
Castrated+anti-IL-6	6	6	6

***N.B.** The above groups used for treatment were selected among many BM18 tumors recipients to standardize tumor volume and growth kinetics; the isotype-matched control antibody had fungal contamination and was therefore not used

In order to conserve precious neutralization antibody and maximize the potential for quantifiable and clinically relevant responses, CNTO328 was used only in combination with androgen deprivation and recipients harvested at later time points with longer-term exposure to antibody therapy. Indeed, it has been suggested that CNTO 328 therapy for prostate cancer could be improved with an additional treatment (e.g. androgen deprivation), yielding a more pronounced effect if antibody treatment was prolonged (Steiner et al., 2006). Once tumors reached ~1cm in diameter, mice to be deprived of androgen underwent surgical castration with a bilateral orchioepididymectomy under isoflurane anesthetic and analgesia (4μg/g mouse, sub-cutaneous injection). Castrated mice undergoing antibody treatment were immediately injected intraperitoneally and weekly thereafter with mouse monoclonal human Interluekin-6 (hIL-6) neutralizing antibody (CNTO 328, 25mg/kg). Tumors were measured on days 4, 6, 7, 8 and 11 post-castration±anti-IL-6 until size remained stable (Fig 1):

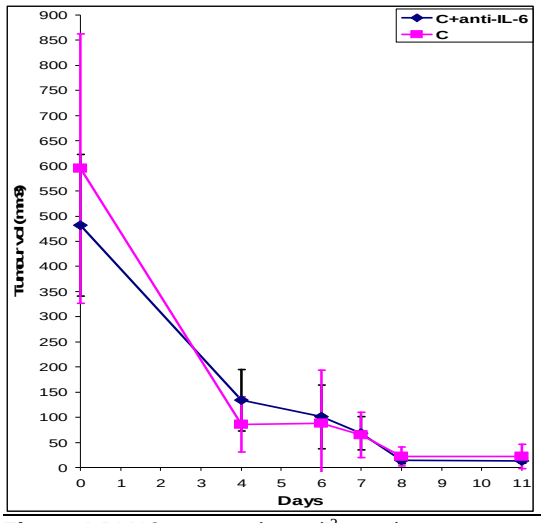

Figure 1 BM18 tumor volume ($l^2/2$ x w) post-castration (C) ± anti-IL-6. n=6

There were no statistically significant differences in tumor volumes between treatment groups during regression and no re-growth was observed in any castrated recipient during the 12-week course of the experiment.

Mice were harvested at 4, 8 and 12 week time points. Portions of each tumor were taken at every time point and snap frozen for analysis of IL-6 pathway molecules. Remaining tumor tissue was processed for routine histology and stained with Masson's Trichome (Fig 2):

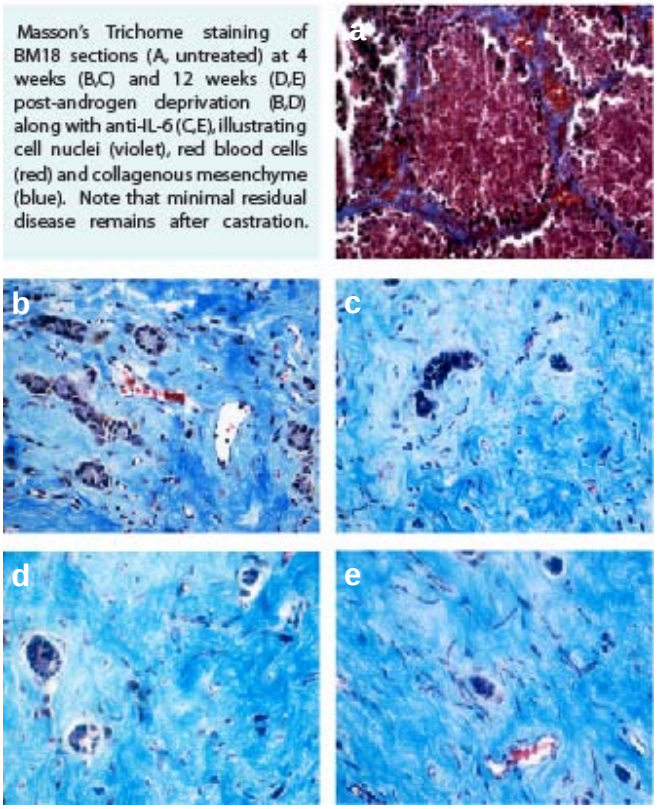

Figure 2 Masson's Trichome staining of BM18 tumors with and without castration±anti-IL-6 at 4 and 12 weeks (8 weeks -- data not shown)

Although a small reduction in cellularity may have been evident at 4 weeks with anti-IL-6 therapy (Fig 2 b vs. c), any difference observed may have been due to small sample size or heterogeneity and in any event was no longer apparent at 12 weeks (d vs. e).

Elevated serum IL-6 levels in prostate cancer patients are closely correlated with tumor burden and are indicative of poor prognosis (Nakashima et al., 2000). SCID mice receiving recombinant human IL-6 or TSU xenografts yielded sera with detectable human IL-6 levels by ELISA (3pg/mL and 30pg/mL, respectively) (Twillie et al., 1995), thereby demonstrating the potential utility of anti-IL-6 therapy and the feasibility of detecting this exogenously produced cytokine when present in mice. Therefore, serum was collected from all BM18 recipients by cardiac puncture upon harvest for the analysis of IL-6 levels by ELISA (BD) as described in Proposal PC050626 (Fig. 3):

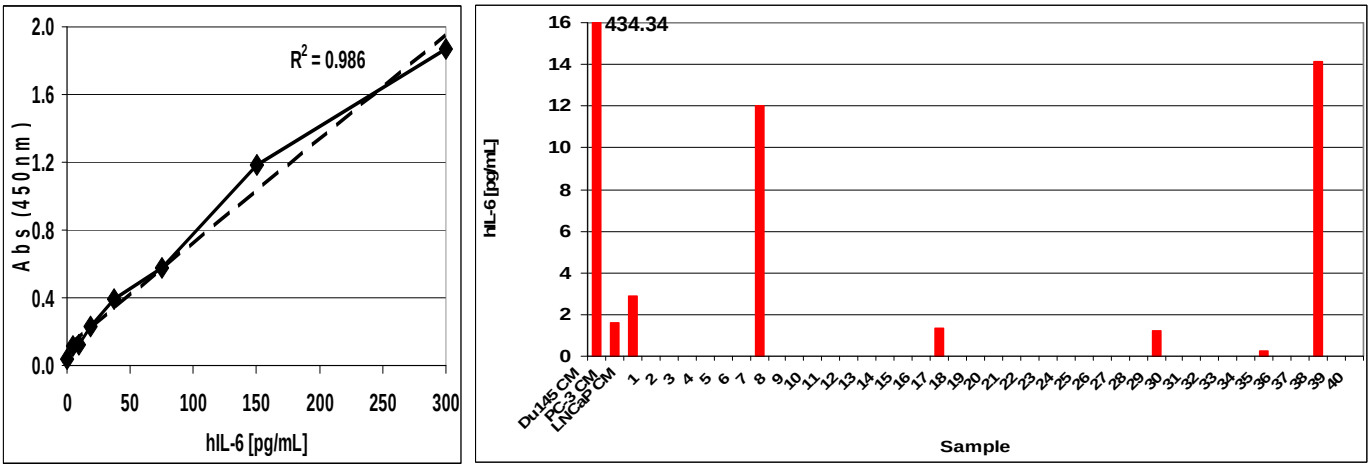

Figure 3 Analysis of human IL-6 levels in sera from BM18 recipients. a) Calibration of the ELISA using purified recombinant hIL-6 indicates successful and precise quantitation. b) Conditioned medium from human prostate cancer cell lines and sera from BM18 samples were measured on the same plate in the same assay.

The human prostate cancer cell lines Du145 (434.34pg/mL) and LNCaP (2.92pg/mL) secreted IL-6 into their media to levels above the threshold of detection (2.2pg/mL, BD OptEIA™ Human IL-6 ELISA Kit II Instruction Manual). Of all BM18 samples from all treatment groups and time points, only samples 7 (castrated, 4weeks; 12.03pg/mL) and 38 (castrated+anti-IL-6, 12 weeks; 14.16pg/mL) exhibited IL-6 serum levels above the threshold of detection. The rarity of detectable IL-6 readings and lack of any correlation between serum IL-6 and treatments may be consistent with little secretion of any appreciable IL-6 by BM18 tumors into the circulatory system of SCID recipients. However, it should be noted that circulating IL-6 may exist in various high molecular weight complexes that include autoantibodies, complement factors C3b and C4b, C-reactive protein, albumin and soluble IL-6R and gp130 (Kovacs, 2001; May et al., 1992; Muller-Newen et al., 1998; Ndubuisi et al., 1998; Pignatti et al., 2003). Importantly, these IL-6 binding partners have been implicated in masking detection of IL-6 in sera with various commercial ELISAs and biological assays (Kovacs, 2001; May et al., 1992; Muller-Newen et al., 1998; Ndubuisi et al., 1998; Pignatti et al., 2003; Twillie et al., 1995). Although the BD ELISA kit utilized was recommended by a fellow researcher due to its flexibility in quantifying IL-6 in various complexes (B. Jenkins, personal communication), the instruction manual includes the caveat that "…soluble receptors, or other binding proteins in specimens has not been thoroughly investigated" and the "possibility of interference cannot be ruled out." In light of this, it would be prudent to assert that the ELISA results confirmed only that free un-bound IL-6 was not detected in most BM18 recipients but that this did not exclude its possible presence in biologically active complexes.

Task 2. To characterize the expression of IL-6 related signaling molecules and apoptosis in archival BM18 tumor tissue:

2a) Carry out Western Immunoblotting from protein extracted from frozen BM18 tumor tissue. Positive controls will include protein extracted from a cohort of readily available prostate cancer cell lines.

Untreated archival BM18 tissues were analyzed in parallel with those generated from the experimental groups in Task 1b and did not exhibit any notable differences from results reported below in Task 2b.

2b) Extract protein from fresh BM18 xenograft tissue collected from each of the experimental groups in Task 1b and examine key components of the IL-6 signaling cascade by Western blot analysis, optimized in Task 1b.

BM18 tumors were harvested from untreated, castrated and castrated+anti-IL-6-treated SCID recipients at 4, 8 and 12 weeks post-treatment. Tissues were snap-frozen in liquid nitrogen, pulverized into powder and the protein extracted in RIPA buffer with protease and phosphatase inhibitors as per manufacturer's instructions (Pierce). The volume for 50μg protein of each sample was determined with the Pierce BCA Assay, prepared in LDS Sample Buffer with Sample Reducing Agent and separated on 4-12% Novex NuPAGE Bis/Tris pre-cast gels in MOPS Running Buffer for 75 minutes at 150V (Invitrogen). Separated proteins were transferred to nitrocellulose membranes in pre-chilled standard transfer buffer (25mM Tris/192mM Glycine/20%MeOH) with stirring at 4°C for 75 minutes at 100V (constant V) using the Bio-Rad Mini Trans-Blot system. Membranes were stained with 0.1%(w/v) Ponceau S/5%(v/v) Acetic acid for 5 minutes to visualize proteins, thereby confirming successful transfer and revealing protein loading (Fig. 4):

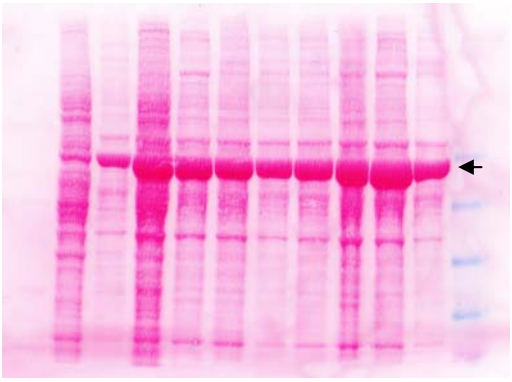

Figure 4 Representative nitrocellulose membrane of 50μg transferred BM18 protein samples visualized with 0.01%(w/v)Ponceau S/0.05%(v/v)Acetic acid. Arrow indicates an abundantly expressed (serum?) protein found only in transplanted tissue.

Ponceau S was washed off by immersion in 0.1M NaOH and the membrane was blocked for 1 hour with Odyssey Blocking Buffer (Li-Cor) prior to overnight incubation at 4°C with the following antibodies (Table II):

Table II Antibodies employed in Western Immunoblots.

Host	Specificity	Target	Manufacturer	Cat. #	Working Dilution	Expected size (kDa)
Mouse	Human/Mouse/ Rat/Rabbit	Pan-actin	Neomarkers	MS-1295-PO	1:5,000	42
Rabbit	Human	IL-6	Santa Cruz	sc-7920	1:100	23/46
Rabbit	Human	pSTAT3(Tyr705)	Cell Signaling Technology	9131S	1:500	79/86
Goat	Human	IL-6	R&D Systems	AF-206-NA	1:500	23/46
Mouse	Human	IL-6R	R&D Systems	MAB227	1:200	80
Goat	Human	p-gp130	Santa Cruz	sc-12978	1:100	130
Rabbit	Human	STAT3	Cell Signaling Technology	9132	1:500	79/86

The antibodies listed in the shaded region of the table represent those that did not yield a detectable or specific signal for their targets. Protein loading of the specific target was possibly too low for detection due to over-representation of the abundantly expressed band at ~50kDa in harvested BM18 tissue (Fig. 4, *arrow*). As the BM18 tumors appeared well vascularized and engorged with blood from the host, it was postulated that the abundant protein likely originated from the host serum. In an attempt to reduce non-specific serum proteins and improve detection, harvested BM18 tumors were minced and washed thoroughly in PBS to remove excess blood prior to snap-freezing and the protein loading was increased to 50μg by concentrating dilute samples if needed, using a cold acetone precipitation protocol (Pierce). In addition, antibody dilutions, detergent concentrations, membrane blocking, membrane washing, transfer buffers, transfer conditions (i.e., voltage and duration) and visualization method (Odyssey Infrared Imaging (Li-Cor) versus chemiluminescence (Supersignal West Femto Maximum Sensitivity Substrate, Pierce)) were all varied in attempts to further optimize detection of the above targets. Although those targets in the shaded region remained elusive, the previously sub-optimal detection of targets IL-6 and pSTAT3(Tyr705) was now remedied to permit robust detection and quantitation of those targets.

In the absence of successful antibody detection of the IL-6 receptors IL-6R and gp130, it was decided to inform our study by determining whether castration±anti-IL-6 therapy elicited any changes in expression of these IL-6 pathway members by using quantitative real-time PCR with SYBR green chemistry on the ABI 7900HT thermal cycler (Fig. 5):

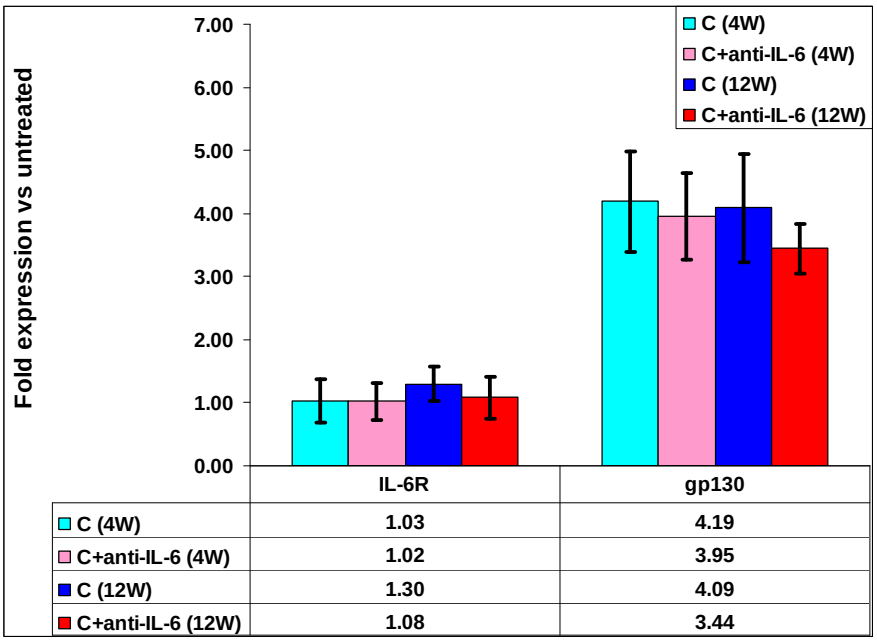

	IL-6R	gp130
C (4W)	1.03	4.19
C+anti-IL-6 (4W)	1.02	3.95
C (12W)	1.30	4.09
C+anti-IL-6 (12W)	1.08	3.44

Figure 5 Analysis of mRNA expression levels of IL-6 pathway members using quantitative real-time PCR. BM18 transplant tissues harvested at 4 and 12 weeks post-castration±anti-IL-6 (C, C+anti-IL-6) were snap frozen, pulverized, and the isolated RNA converted to cDNA with human gene-specific primers. Tumor samples from treated recipients were compared to untreated BM18 tissue. Melt-curves for amplified products were analyzed to confirm synthesis of single specific products with the expected melting temperature and PCR products were run on high resolution agarose gels to confirm synthesis of single products of the expected length (data not shown) as per the Manufacturer's recommendations (Applied Biosystems). Relative expression (**a, b**) was calculated using the $\Delta\Delta C_T$ method (Winer et al., 1999); statistical significance was calculated using a paired or unpaired student's *t*-test (Kirkman, 1996), where data sets had equal or unequal replicates, respectively. Changes from 4 to 12 weeks (**c**) were calculated by dividing 12-week relative expression by the corresponding 4 week values. C (4W): *n*=4; C+anti-IL-6 (4W): *n*=6; C, C+anti-IL-6 (12W):*n*=3.

Expression of IL-6R mRNA transcripts was detected in BM18 tumors of treated and untreated recipients, confirming competence to respond to IL-6-initiated signaling as previously reported in Proposal PC050626. However, the IL-6R mRNA levels did not differ between treated and untreated or between anti-IL-6 treated and non-antibody treated castrated recipients (Fig. 5). While any changes in IL-6R expression resulting from CNTO 328 would have provided strong presumptive evidence of IL-6-specific effects, the absence of difference neither confirmed nor excluded this possibility.

Recruitment and phosphorylation of the signal-transducing receptor gp130 occurs upon engagement of various IL-6-type cytokines with their respective receptors. Those that can initiate signaling via gp130 include IL-6, IL-11, LIF, CT-1, CNTF and OSM (Heinrich et al., 1998). Notably, BM18 tumors of all castrated recipients exhibited large increases in gp130 expression levels. This would be consistent with IL-6-type cytokine signaling via STATs, as STAT1 and STAT3 homo- and heterodimers initiate transcription of gp130 (O'Brien and Manolagas, 1997). However, there was no difference when IL-6

neutralizing antibody was administered, implicating one of the other aforementioned IL-6-type cytokines in raising gp130 levels via STAT activation.

Determining whether the treatment regime elicited any changes to protein levels of IL-6 -- the cytokine at the apex of the signaling cascade under study -- and phosphoSTAT3 – the effector molecule at the terminus – was of paramount importance to establish the efficacy of anti-IL-6 therapy and the importance of IL-6 signaling in the BM18 xenograft model. Western Immunoblotting was optimized to detect these critical mediators of the IL-6 pathway (Fig. 6):

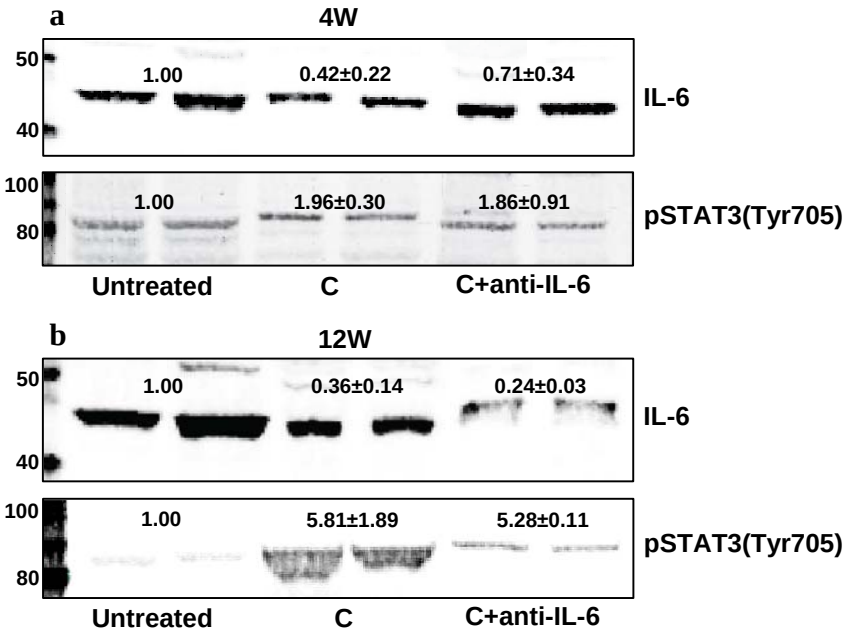

Figure 6 Western Immunoblot detection of IL-6 and phospho-STAT3(Tyr705). Tumors from untreated, castrated (C) and castrated+anti-IL-6-treated (C+anti-IL-6) recipients of BM18 xenografts were harvested at 4 weeks (a) and 12 weeks (b) post-castration±anti-IL-6 therapy. Expression of IL-6 was detected with rabbit anti-human IL-6 (1:100, Santa Cruz, Cat. sc-12978) and pSTAT3 was detected with rabbit anti-human pSTAT3(Tyr705) (1:500, Cell Signaling Technology, Cat. 9131S). Odyssey Blocking Buffer (Li-Cor)/0.05%(v/v) Tween-20 was used for antibody dilution and washing of membranes. Mouse anti-pan-actin (1:5,000, Neomarkers, Cat. MS-1295-PO) was utilized for normalization of protein loading (data not shown). Goat anti-rabbit IRDye800W (1:2,500, Rockland, Cat. 605-431-013) and Goat anti-mouse AlexaFluor 680 (1:5,000, Molecular Probes) secondary antibodies were utilized to detect primary antibody-bound IL-6 and pSTAT3 or pan-actin, respectively. Targets were visualized on the Odyssey Infrared Imaging System and quantitated on the Odyssey Application Software (Version 1.2.15, Li-Cor).

Under partially denaturing conditions, IL-6 may appear to be a 43-45-kDa un-reduced homodimer by Western Immunoblotting (Fong et al., 1989; Jablons et al., 1989; Santhanam et al., 1989). The results in this study were consistent with this, as the band corresponding to IL-6 exhibited a molecular mass of ~46kDa (Fig. 6). At 4 weeks post-castration, regressed BM18 tumors from castrated hosts with or

without anti-IL-6 therapy exhibited a reduction in IL-6 protein (Fig. 6a, upper). Although the antibody-treated tissue appeared to express slightly higher levels of IL-6 at 4 weeks, the differences were not statistically significant (p=0.15). By 12 weeks, IL-6 levels in tumors of anti-IL-6-treated recipients were reduced ~3-fold as compared to the corresponding treatment group at 4 weeks (Fig. 6b, upper), and this was virtually statistically significant (p=0.057). However, there was no statistically significant difference in tumor IL-6 levels between castrated recipients with or without anti-IL-6 therapy (p=0.28), nor was there any significant difference in castrate-only recipients from 4 to 12 weeks (p=0.67). In short, though IL-6 protein levels appeared lower upon castration and trended downward with time in all treatment groups, anti-IL-6 therapy did not have a significant additional impact.

Despite the apparent lack of significant effects upon total tumor IL-6 protein levels with anti-IL-6 therapy, it remained possible that free un-bound and potentially active IL-6 was confined to cell cytosols while secreted IL-6 was sequestered by CNTO 328, thereby preventing IL-6-induced paracrine signaling regardless of total tumor IL-6 protein levels. If there was a biological effect upon IL-6 signaling elicited by anti-IL-6 therapy, it would likely be manifest in a concomitant reduction of activated (phosphorylated) STAT3, an effector molecule that ultimately transduces IL-6 signals to regulate gene transcription via acute-phase response elements (Lutticken et al., 1994; Stahl et al., 1994). STAT proteins are ubiquitously expressed and their regulation at the transcript level is not important in cytokine signaling (Heinrich et al., 1998). The critical hallmark of cytokine signaling is phosphorylation of STAT. Upon engagement of IL-6 with its receptors and recruitment of Janus kinases, STAT3 is recruited for phosphorylation at tyrosine residue 705 (Tyr705) which induces dimerization, followed by translocation to the nucleus and DNA binding (Darnell et al., 1994; Ihle, 1995). Importantly, while IL-6-stimulated activation of STAT3 in benign cells is transient, elevated levels of constitutively activated STAT3 are associated with cancerous prostate and are significantly correlated with more aggressive disease (Barton et al., 2004; Campbell et al., 2001; Mora et al., 2002). By 4 weeks post-castration, BM18 tumors exhibited an almost 2-fold increase in the active form of STAT3, pSTAT3(Tyr705), regardless of whether IL-6 neutralization was employed (Fig. 6a, lower). Ominously, by 12 weeks, activated STAT3 was even more elevated (>5-fold) in tumors after castration as compared to untreated BM18 tumors (Fig. 6b, lower) and the increase during that period in each corresponding treatment group was statistically significant (castrated 4 vs 12 weeks, p=0.0032; castrated+anti-IL-6, 4 vs 12 weeks, p=0.0004). CNTO 328 treatment of castrated BM18 recipients did not induce any statistically significant reduction in pSTAT3 as compared to samples from castrated recipients with no anti-IL-6 therapy at 12 weeks (p=0.66). Taken together, the IL-6R and gp130 mRNA

expression levels and IL-6 and pSTAT3 Western Immunoblot data suggest that either the CNTO 328 antibody lacked efficacy in the BM18 xenograft model or that IL-6-initiated signaling is not a critical feature of BM18 tumor biology in the context of this experiment. Given the significant increases in gp130 expression and activated STAT3 protein in the absence of changes to IL-6 and IL-6R with anti-IL-6 therapy, it is likely that some other IL-6-type family cytokine was responsible for signaling via gp130 and STAT3, e.g. IL-11, LIF, CT-1, CNTF or OSM.

2c) Measure apoptosis and cellular proliferation in formalin fixed paraffin embedded BM18 xenograft tissue sections also collected from each of the experimental groups in Task 1b.

This task was approached with an alternative methodology to rapidly generate results that could potentially inform our analyses and add novelty to our study. The expression levels of various mRNA targets (Table III), including apoptosis (Bcl-2) and proliferation (CD71) markers, and indicators of prostate cancer progression and aggressiveness (PSA, AR, NSE), were measured using quantitative real-time PCR as described above (Fig. 7).

Table III mRNA transcripts analyzed by quantitative real-time PCR

Target	Rationale
Bcl-2	• Associated with the emergence of androgen-independent prostate cancer (McDonnell et al., 1992) and progression to metastatic disease (Furuya et al., 1996) • Protein levels of Bcl-2 decreased by CNTO 328 (Steiner et al., 2006)
CD71	• Widely expressed by actively proliferating cells (Taetle, 1990; Tani et al., 2000) • Proliferating prostate-cancer cells express high levels of CD71 (Keer et al., 1990)
PSA	• PSA secretion into bloodstream 10-fold higher in prostate cancer than benign tissue (Stamey et al., 1987) • PSA levels proportional to volume of prostate cancer present in 90% of cases (Catalona and Loeb, 2005) • PSA levels directly correlated to prostate cancer aggressiveness (Antenor et al., 2005)
AR	• Increases in AR mRNA and protein necessary and sufficient for conversion of prostate cancer growth from androgen-dependent to hormone-refractory (Chen et al., 2004)
NSE	• Neuroendocrine (NE) differentiation a more reliable prognostic indicator than conventional grading systems (Cohen et al., 1991; Weinstein et al., 1996) • NE (neuron-specific enolase, NSE^+) cell population increased in tumor foci and correlates with tumor progression, poor prognosis, and hormone refractory prostate cancer (di Sant'Agnese, 1992)

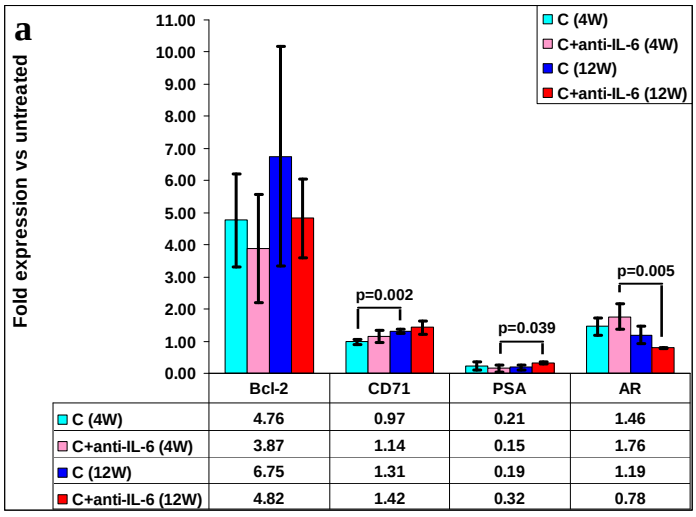

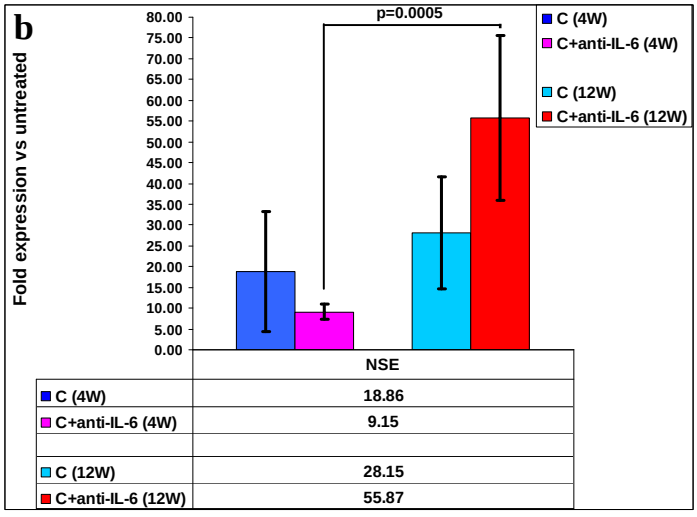

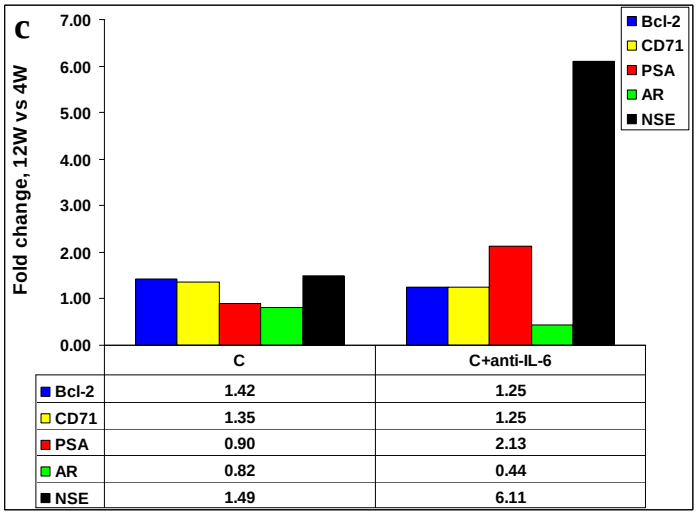

Figure 7 Analysis of mRNA expression levels of various targets using quantitative real-time PCR. BM18 transplant tissues harvested at 4 and 12 weeks post-castration±anti-IL-6 (C, C+anti-IL-6) were snap frozen, pulverized, and the isolated RNA converted to cDNA with human gene-specific primers. Tumor samples from treated recipients were compared to untreated BM18 tissue. Melt-curves for amplified products were analyzed to confirm synthesis of single specific products with the expected melting temperature and PCR products were run on high resolution agarose gels to confirm synthesis of single products of the expected length (data not shown) as per the Manufacturer's recommendations (Applied Biosystems). Relative expression (**a, b**) was calculated using the $\Delta\Delta C_T$ method (Winer et al., 1999); statistical significance was calculated using a paired or unpaired student's *t*-test (Kirkman, 1996), where data sets had equal or unequal replicates, respectively. Changes from 4 to 12 weeks (**c**) were calculated by dividing 12-week relative expression by the corresponding 4 week values. C (4W): *n*=4; C+anti-IL-6 (4W): *n*=6; C, C+anti-IL-6 (12W):*n*=3.

Not unexpectedly, Bcl-2 expression in regressed tumors was elevated, suggesting a possible mechanism for their escape from apoptosis after androgen withdrawal (Fig. 7a). This survival protein is another pSTAT3 target (Nielsen et al., 1999; Real et al., 2002), and its increase may be attributed to upregulation of activated STAT3 as detected by Western Immunoblot (refer to Fig. 6).

Screening of serum for increases in prostate-specific antigen (PSA) attributed exclusively to prostatic epithelial cells, has been a front-line diagnostic measure of prostatic disease for nearly 20 years (Catalona et al., 1991). By this measure, regressed BM18 tumors in castrated recipients had a lower total disease burden as would be expected with much lower total cell numbers and cellularity. Though it remained below levels in tumors from untreated mice in all treatment groups for the duration of the

experiment and there were no significant differences with CNTO 328 administration, the increase from 4 to 12 weeks with anti-IL-6 therapy was statistically significant (p=0.039). Rising PSA levels with time are considered a prognostic indicator of future disease recurrence (Carter et al., 1992), hence, continuation of this trend over time would be consistent with eventual disease recurrence.

The dramatic increase in the neuroendocrine marker neuron-specific enolase (NSE) in castrated prostate tumor recipients (Fig. 7b) is consistent with numerous studies where investigators reported neuroendocrine differentiation upon androgen withdrawal (Ismail et al., 2002; Ito et al., 2001; Jongsma et al., 1999). It has also been reported that differentiation toward this lineage increases with time after androgen ablation therapy (Ito et al., 2001). The current study corroborates these observations, as both treatment groups exhibited marked increases in NSE expression compared to untreated BM18 tumors, and the increases became even more pronounced from 4 to 12 weeks post-castration (Fig. 7b). Importantly, as was the case for PSA, the anti-IL-6-treated BM18 tumors demonstrated a statistically significant increase in NSE during the course of the experiment from ~19-fold versus untreated tumors at 4 weeks to ~56-fold at 12 weeks (Fig. 7b), representing a ~6-fold increase (Fig. 7c). Given the rationale for analysis of PSA and NSE (i.e., poor prognostic indicators – refer to Table III), these critical observations suggest that anti-IL-6 therapy of BM18 or similar prostate tumors may actually accelerate progression of disease toward a hormone-refractory incurable cancer.

It has been reported that CNTO 328 treatment in another human prostate xenograft model yielded a reduction in proliferative cells, as indicated by Ki-67 immunoreactivity (Steiner et al., 2006). In light of the lack of re-growth of regressed BM18 tumors after castration, it would be expected that expression of another robust marker of proliferation (CD71) would also be reduced, perhaps more so with CNTO 328 administration. However, this was not the case. In fact, there was a slight increase in expression with anti-IL therapy, and an increase with time in both treatment groups (Fig. 7a). Previous studies have demonstrated that neoplastic NE cells are non-proliferative and the aggressiveness of the ensuing cancerous growth can be attributed to their paracrine stimulation of adjacent non-NE cells (Bonkhoff et al., 1995; Bonkhoff et al., 1991). These observations may explain why there was a slight increase in the expression of the proliferation-associated CD71 during the course of the experiment (Fig. 7c) despite the apparent increase in non-proliferative neuroendocrine character. Possibly, any significant CD71 increase in adjacent non-NE cells resulting from paracrine stimulation may have been masked by the dominance of the non-proliferative NE cells in the sample or even dampened by CNTO 328 administration.

It has been demonstrated that NE cells lack detectable AR (Bonkhoff et al., 1993; Krijnen et al., 1993), suggesting these cells are hormone-refractory (Bonkhoff, 1998). The statistically significant reduction in AR and concomitant increase in NSE expression observed in tumors of IL-6-treated mice from 4 to 12 weeks (Fig. 7a) is consistent with this and suggests progression towards androgen independence. Indeed, the very survival of cells in regressed tumors of castrated hosts is strong presumptive evidence of their hormone-refractory status. However, the presence of AR expression in what may be predominantly neuroendocrine tissue suggests the maintenance of a non-NE cell population within these tumors. The presence of potentially proliferative hormone-responsive cells among these hormone-refractory non-proliferative cells in regressed BM18 tumors has been confirmed previously, as evidenced by robust re-growth upon exogenous androgen replacement (E. Williams, unpublished observations). Precisely why BM18 tumors in castrated±anti-IL-6-treated recipients with dominant neuroendocrine character and potentially proliferative $CD71^{+}$ cells did not progress to androgen-independent re-growth during this experiment is unknown, but may have been due to the relatively short time-frame or elusive stimuli that were absent due to inter-species incompatibility between human tumor and mouse stromal cells.

Aim 2. Describe the IL-6 signaling cytokines and their respective receptors in human prostate cancer bone metastases.

Task 1. To characterize key components of the IL-6 axis in PrCa bone metastases from patient biopsies, i.e. examining which cells express particular proteins of the axis:

1a) To perform immunohistochemistry on formalin-fixed, paraffin wax embedded PrCa bone metastasis tumors obtained from PrCa patient biopsies (currently n=40) to examine the expression and localization of the IL-6 family of cytokines and their respective receptors.

While expression and localization of IL-6 and gp130 has been studied in organ-confined PrCa, the key mediators of the IL-6/gp130 signaling pathway have not been previously assessed in prostatic bone metastases. We therefore examined a cohort of 14 bone metastases from human patients for expression and localization of IL-6, IL-6R and phospho-gp130 using immunohistochemistry.

Table IV Average frequency of cells positive for IL-6R, phospho-gp130 and IL-6 in human bone metastasis samples.

Sample	IL-6R	phospho-gp130	IL-6
BM19	100	97	88
BM21	85	98	77
03R56	93	72	87
BM11	71	97	60
155938	100	27	98
BM5	61	75	75
244210	92	20	93
958580	97	25	80
BM18b	67	67	63
BM7	59	63	37
BM8	0	64	82
193970b	0	77	59
180606B	21	0	88
169463	0	1	98

All cells in all fields of at least three sections from each patient biopsy were scored for the frequency of IL-6R, phospho-130 and IL-6 positive cells.

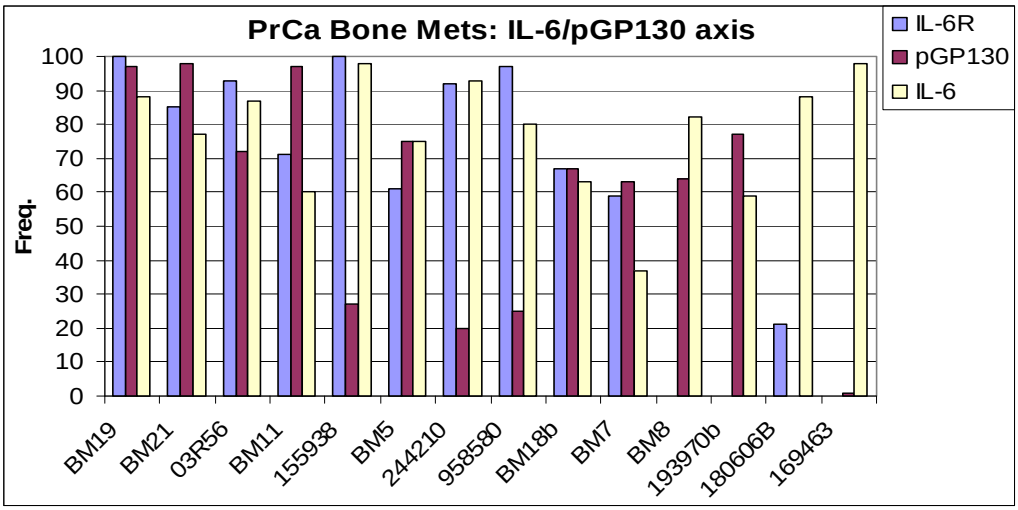

Figure 8 Frequency of cells positive for IL-6R, pGP130 (phospho-gp130) and IL-6 in human patient bone metastasis biopsies.

Our investigations with archival patient biopsies have revealed that all PrCa bone metastases examined (*n*=14) expressed IL-6 on an overwhelming majority of cells (78±5%). The IL-6 receptor was expressed in 11/14 cases by 77±7% of PrCa cells. Activated phospho-gp130 was expressed in all but one case (13/14), and was expressed in the majority of cells (79±5%) in 9/14 cases. Thus, members of the IL-6/gp130 axis are present in a high proportion of bone metastatic PrCa cells in most cases.

To measure the overall expression levels of these markers within the bone metastasis samples, all cells within all fields of at least three sections of each biopsy were scored from 0-3 with respect to staining intensity and the results averaged (Table V, Fig. 9).

Table V Average intensity of IL-6R, phospho-gp130 and IL-6 staining in human bone metastasis samples.

Sample	IL-6R	phospho-gp130	IL-6
03R56	59	36	57
958580	57	8	66
155938	37	10	81
244210	58	7	60
BM19	38	35	52
BM5	26	48	51
BM21	29	33	42
BM11	26	34	43
BM18b	27	22	45
BM8	0	22	53
193970b	0	46	23
180606B	13	0	54
BM7	20	24	21
169463	0	0	61

Cells with no signal were scored with intensity = 0. All positive cells were scored from 1 (low) to 3 (high). To calculate a measure of average overall intensity for each marker, the frequency of positive cells with a given intensity was multiplied by that intensity and the frequency-intensity products for the degrees of intensity 1-3 were averaged. For example, in scoring the intensity of IL-6R in sample 03R56, it was found that 40% of positive cells were intensity = 3 (40 x 3), 5% of positive cells were 2 (5 x 2) and 48% of positive cells were scored 1 (48 x 1). Therefore, the average overall intensity is calculated as ((40 x 3) + (5 x 2) + (48 x 1)) / 3 = 59 of a possible 100 (Table V, *row 2, column 2*).

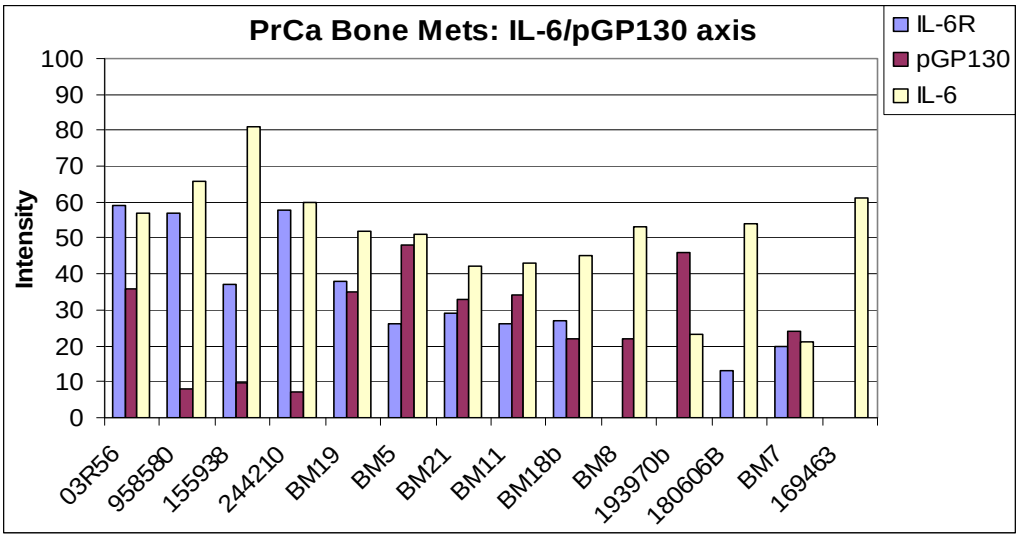

Figure 9 Intensity of staining in cells positive for IL-6R, pGP130 (phospho-gp130) and IL-6 in human bone metastasis samples.

For IL-6R, the overall average intensity of positive cells in all samples was 35±16 of a possible 100. For phospho-gp130, the overall average intensity of positive cells in all samples was 27±14 of a possible 100, and for IL-6 the overall average intensity of positive cells was 51±16 of a possible 100. Clearly, significant levels of IL-6R, phospho-gp130 and IL-6 were present in this cohort of bone metastases. Together with the high frequency of expression of these markers, these data provide strong presumptive evidence that the IL-6/gp130 signaling axis is an important pathway in prostate cancer bone metastases.

Key Research Accomplishments

- Successfully performed harvest and serial transplantation of BM18 xenografts into SCID mouse recipients
- Developed high-throughput method of assaying protein concentration in 96-well plate format using BMG Labtech's FLUOStar Optima fluorescent plate reader
- Achieved competency in SDS-PAGE and Western Immunoblotting techniques
- Achieved competency in near-infrared fluorescent detection of Western Immunoblot targets with visualization on the Li-Cor Odyssey imaging system
- Achieved competency in visualization of Western Immunoblot targets using the Pierce Biotechnology SuperSignal West Femto Chemiluminescence system
- Optimized detection of pan-actin, IL-6, sIL-6R and STAT3 in PrCa cell lines and IL-6 and pSTAT3(Tyr705) in BM18 xenograft tissue by Western Immunoblotting
- Characterized frequency and intensity of IL-6R, phospho-gp130 and IL-6 expression in a cohort of human prostate cancer bone metastases that to our knowledge has only ever been reported in organ-confined prostate cancer
- Provided further evidence implicating IL-6 signaling in bone-metastatic prostate cancer
- Characterized response to anti-IL-6 therapy in a hormone-dependent prostate cancer xenograft, thereby implicating other IL-6-type cytokines in increased gp130 and pSTAT3
- Provided further evidence that androgen deprivation therapy induces increases in survival protein Bcl-2, prognostic marker PSA and neuroendocrine differentiation and may therefore create the pre-conditions for a much more dangerous hormone-refractory disease recurrence

Reportable Outcomes

Abstracts/presentations:

Sep 2007 Department of Defense IMPaCT (Innovative Minds in Prostate Cancer Today) meeting, Atlanta, GA, U.S.A. *Poster presentation*

Feb 2008 Lorne Cancer Conference, Lorne, Victoria, Australia. *Poster presentation*

Employment or research opportunities applied for and/or received based on experience/training supported by this grant:

Mar 2008 National Breast Cancer Foundation (NBCF, Australia) Postdoctoral Fellowship, Cancer Biology Laboratory, Peter MacCallum Cancer Centre, East Melbourne, Victoria, Australia.

Oct 2008 Ramaciotti Foundation Establishment Grant ($30,000)

Conclusion

Collectively, the data presented herein demonstrate that while IL-6 signaling is implicated in many cases of aggressive bone-metastatic prostate cancer, there is no compelling proof that IL-6 is a critical determinant in BM18 growth or survival in the current experimental context. This is consistent with a previous study where hormone-responsive and PSA-secreting prostate cancer cell lines did not secrete detectable IL-6 as measured by ELISA (Twillie et al., 1995), although limitations of detection must be considered (refer to Fig. 3 discussion). It has been noted previously that anti-IL-6 therapy for IL-6-secreting prostate cancer xenografts has yielded mixed results, with one responding and two others refractory (Smith and Keller, 2001; Zaki et al., 2004). This and other data led to the suggestion that targeting IL-6 with antibodies may ameliorate only a subset of prostate cancers (Steiner et al., 2006) and perhaps BM18 is not one of them.

Significantly, this study has corroborated a growing literature suggesting that androgen deprivation therapy induces neuroendocrine differentiation and other changes that yield a potentially much more dangerous phenotype, increasing the likelihood of hormone-refractory disease emerging in the future.

References

1. Antenor, J.A., Roehl, K.A., Eggener, S.E., Kundu, S.D., Han, M., and Catalona, W.J. (2005). Preoperative PSA and progression-free survival after radical prostatectomy for Stage T1c disease. Urology *66*, 156-160.
2. Barton, B.E., Karras, J.G., Murphy, T.F., Barton, A., and Huang, H.F. (2004). Signal transducer and activator of transcription 3 (STAT3) activation in prostate cancer: Direct STAT3 inhibition induces apoptosis in prostate cancer lines. Molecular cancer therapeutics *3*, 11-20.
3. Bonkhoff, H. (1998). Neuroendocrine cells in benign and malignant prostate tissue: morphogenesis, proliferation, and androgen receptor status. Prostate Suppl *8*, 18-22.
4. Bonkhoff, H., Stein, U., and Remberger, K. (1993). Androgen receptor status in endocrine-paracrine cell types of the normal, hyperplastic, and neoplastic human prostate. Virchows Arch A Pathol Anat Histopathol *423*, 291-294.
5. Bonkhoff, H., Stein, U., and Remberger, K. (1995). Endocrine-paracrine cell types in the prostate and prostatic adenocarcinoma are postmitotic cells. Hum Pathol *26*, 167-170.
6. Bonkhoff, H., Wernert, N., Dhom, G., and Remberger, K. (1991). Relation of endocrine-paracrine cells to cell proliferation in normal, hyperplastic, and neoplastic human prostate. The Prostate *19*, 91-98.
7. Campbell, C.L., Jiang, Z., Savarese, D.M., and Savarese, T.M. (2001). Increased expression of the interleukin-11 receptor and evidence of STAT3 activation in prostate carcinoma. The American journal of pathology *158*, 25-32.
8. Carter, H.B., Pearson, J.D., Metter, E.J., Brant, L.J., Chan, D.W., Andres, R., Fozard, J.L., and Walsh, P.C. (1992). Longitudinal evaluation of prostate-specific antigen levels in men with and without prostate disease. JAMA *267*, 2215-2220.
9. Catalona, W.J., and Loeb, S. (2005). The PSA era is not over for prostate cancer. Eur Urol *48*, 541-545.
10. Catalona, W.J., Smith, D.S., Ratliff, T.L., Dodds, K.M., Coplen, D.E., Yuan, J.J., Petros, J.A., and Andriole, G.L. (1991). Measurement of prostate-specific antigen in serum as a screening test for prostate cancer. N Engl J Med *324*, 1156-1161.
11. Chen, C.D., Welsbie, D.S., Tran, C., Baek, S.H., Chen, R., Vessella, R., Rosenfeld, M.G., and Sawyers, C.L. (2004). Molecular determinants of resistance to antiandrogen therapy. Nat Med *10*, 33-39.

12. Cohen, R.J., Glezerson, G., and Haffejee, Z. (1991). Neuro-endocrine cells--a new prognostic parameter in prostate cancer. Br J Urol *68*, 258-262.
13. Darnell, J.E., Jr., Kerr, I.M., and Stark, G.R. (1994). Jak-STAT pathways and transcriptional activation in response to IFNs and other extracellular signaling proteins. Science (New York, NY *264*, 1415-1421.
14. di Sant'Agnese, P.A. (1992). Neuroendocrine differentiation in human prostatic carcinoma. Hum Pathol *23*, 287-296.
15. Fong, Y., Moldawer, L.L., Marano, M., Wei, H., Tatter, S.B., Clarick, R.H., Santhanam, U., Sherris, D., May, L.T., Sehgal, P.B., *et al.* (1989). Endotoxemia elicits increased circulating beta 2-IFN/IL-6 in man. J Immunol *142*, 2321-2324.
16. Furuya, Y., Krajewski, S., Epstein, J.I., Reed, J.C., and Isaacs, J.T. (1996). Expression of bcl-2 and the progression of human and rodent prostatic cancers. Clin Cancer Res *2*, 389-398.
17. Heinrich, P.C., Behrmann, I., Muller-Newen, G., Schaper, F., and Graeve, L. (1998). Interleukin-6-type cytokine signalling through the gp130/Jak/STAT pathway. Biochem J *334 (Pt 2)*, 297-314.
18. Ihle, J.N. (1995). Cytokine receptor signalling. Nature *377*, 591-594.
19. Ismail, A.H.R., Landry, F., Aprikian, A.G., and Chevalier, S. (2002). Androgen ablation promotes neuroendocrine cell differentiation in dog and human prostate. The Prostate *51*, 117-125.
20. Ito, T., Yamamoto, S., Ohno, Y., Namiki, K., Aizawa, T., Akiyama, A., and Tachibana, M. (2001). Up-regulation of neuroendocrine differentiation in prostate cancer after androgen deprivation therapy, degree and androgen independence. Oncol Rep *8*, 1221-1224.
21. Jablons, D.M., Mule, J.J., McIntosh, J.K., Sehgal, P.B., May, L.T., Huang, C.M., Rosenberg, S.A., and Lotze, M.T. (1989). IL-6/IFN-beta-2 as a circulating hormone. Induction by cytokine administration in humans. J Immunol *142*, 1542-1547.
22. Jongsma, J., Oomen, M.H., Noordzij, M.A., Van Weerden, W.M., Martens, G.J., van der Kwast, T.H., Schroder, F.H., and van Steenbrugge, G.J. (1999). Kinetics of neuroendocrine differentiation in an androgen-dependent human prostate xenograft model. The American journal of pathology *154*, 543-551.
23. Keer, H.N., Kozlowski, J.M., Tsai, Y.C., Lee, C., McEwan, R.N., and Grayhack, J.T. (1990). Elevated transferrin receptor content in human prostate cancer cell lines assessed in vitro and in vivo. J Urol *143*, 381-385.
24. Kirkman, T.W. (1996). Statistics to use. http://www.physics.csbsju.edu/stats/. 10 Oct 2008.

25. Kovacs, E. (2001). Investigation of interleukin-6 (IL-6), soluble IL-6 receptor (sIL-6R) and soluble gp130 (sgp130) in sera of cancer patients. Biomedicine & pharmacotherapy = Biomedecine & pharmacotherapie *55*, 391-396.
26. Krijnen, J.L., Janssen, P.J., Ruizeveld de Winter, J.A., van Krimpen, H., Schroder, F.H., and van der Kwast, T.H. (1993). Do neuroendocrine cells in human prostate cancer express androgen receptor? Histochemistry *100*, 393-398.
27. Lutticken, C., Wegenka, U.M., Yuan, J., Buschmann, J., Schindler, C., Ziemiecki, A., Harpur, A.G., Wilks, A.F., Yasukawa, K., Taga, T., *et al.* (1994). Association of transcription factor APRF and protein kinase Jak1 with the interleukin-6 signal transducer gp130. Science (New York, NY *263*, 89-92.
28. May, L.T., Viguet, H., Kenney, J.S., Ida, N., Allison, A.C., and Sehgal, P.B. (1992). High levels of "complexed" interleukin-6 in human blood. The Journal of biological chemistry *267*, 19698-19704.
29. McCulloch, D.R., Opeskin, K., Thompson, E.W., and Williams, E.D. (2005). BM18: A novel androgen-dependent human prostate cancer xenograft model derived from a bone metastasis. The Prostate *65*, 35-43.
30. McDonnell, T.J., Troncoso, P., Brisbay, S.M., Logothetis, C., Chung, L.W., Hsieh, J.T., Tu, S.M., and Campbell, M.L. (1992). Expression of the protooncogene bcl-2 in the prostate and its association with emergence of androgen-independent prostate cancer. Cancer research *52*, 6940-6944.
31. Mora, L.B., Buettner, R., Seigne, J., Diaz, J., Ahmad, N., Garcia, R., Bowman, T., Falcone, R., Fairclough, R., Cantor, A., *et al.* (2002). Constitutive activation of Stat3 in human prostate tumors and cell lines: direct inhibition of Stat3 signaling induces apoptosis of prostate cancer cells. Cancer research *62*, 6659-6666.
32. Muller-Newen, G., Kuster, A., Hemmann, U., Keul, R., Horsten, U., Martens, A., Graeve, L., Wijdenes, J., and Heinrich, P.C. (1998). Soluble IL-6 receptor potentiates the antagonistic activity of soluble gp130 on IL-6 responses. J Immunol *161*, 6347-6355.
33. Nakashima, J., Tachibana, M., Horiguchi, Y., Oya, M., Ohigashi, T., Asakura, H., and Murai, M. (2000). Serum interleukin 6 as a prognostic factor in patients with prostate cancer. Clin Cancer Res *6*, 2702-2706.
34. Ndubuisi, M.I., Patel, K., Rayanade, R.J., Mittelman, A., May, L.T., and Sehgal, P.B. (1998). Distinct classes of chaperoned IL-6 in human blood: differential immunological and biological availability. J Immunol *160*, 494-501.

35. Nielsen, M., Kaestel, C.G., Eriksen, K.W., Woetmann, A., Stokkedal, T., Kaltoft, K., Geisler, C., Ropke, C., and Odum, N. (1999). Inhibition of constitutively activated Stat3 correlates with altered Bcl-2/Bax expression and induction of apoptosis in mycosis fungoides tumor cells. Leukemia *13*, 735-738.
36. O'Brien, C.A., and Manolagas, S.C. (1997). Isolation and characterization of the human gp130 promoter. Regulation by STATS. The Journal of biological chemistry *272*, 15003-15010.
37. Pignatti, P., Ciapponi, L., Galle, P., Hansen, M.B., Massa, M., Meazza, C., Paonessa, G., Novick, D., Ciliberto, G., Martini, A., *et al.* (2003). High circulating levels of biologically inactive IL-6/SIL-6 receptor complexes in systemic juvenile idiopathic arthritis: evidence for serum factors interfering with the binding to gp130. Clinical and experimental immunology *131*, 355-363.
38. Real, P.J., Sierra, A., De Juan, A., Segovia, J.C., Lopez-Vega, J.M., and Fernandez-Luna, J.L. (2002). Resistance to chemotherapy via Stat3-dependent overexpression of Bcl-2 in metastatic breast cancer cells. Oncogene *21*, 7611-7618.
39. Santhanam, U., Ghrayeb, J., Sehgal, P.B., and May, L.T. (1989). Post-translational modifications of human interleukin-6. Arch Biochem Biophys *274*, 161-170.
40. Smith, P.C., and Keller, E.T. (2001). Anti-interleukin-6 monoclonal antibody induces regression of human prostate cancer xenografts in nude mice. The Prostate *48*, 47-53.
41. Stahl, N., Boulton, T.G., Farruggella, T., Ip, N.Y., Davis, S., Witthuhn, B.A., Quelle, F.W., Silvennoinen, O., Barbieri, G., Pellegrini, S., *et al.* (1994). Association and activation of Jak-Tyk kinases by CNTF-LIF-OSM-IL-6 beta receptor components. Science (New York, NY *263*, 92-95.
42. Stamey, T.A., Yang, N., Hay, A.R., McNeal, J.E., Freiha, F.S., and Redwine, E. (1987). Prostate-specific antigen as a serum marker for adenocarcinoma of the prostate. N Engl J Med *317*, 909-916.
43. Steiner, H., Cavarretta, I.T., Moser, P.L., Berger, A.P., Bektic, J., Dietrich, H., Zaki, M.H., Nakada, M., Hobisch, A., Nemeth, J.A., *et al.* (2006). Regulation of growth of prostate cancer cells selected in the presence of interleukin-6 by the anti-interleukin-6 antibody CNTO 328. The Prostate *66*, 1744-1752.
44. Taetle, R. (1990). The role of transferrin receptors in hemopoietic cell growth. Exp Hematol *18*, 360-365.
45. Tani, H., Morris, R.J., and Kaur, P. (2000). Enrichment for murine keratinocyte stem cells based on cell surface phenotype. Proceedings of the National Academy of Sciences of the United States of America *97*, 10960-10965.

46. Twillie, D.A., Eisenberger, M.A., Carducci, M.A., Hseih, W.S., Kim, W.Y., and Simons, J.W. (1995). Interleukin-6: a candidate mediator of human prostate cancer morbidity. Urology *45*, 542-549.
47. Weinstein, M.H., Partin, A.W., Veltri, R.W., and Epstein, J.I. (1996). Neuroendocrine differentiation in prostate cancer: enhanced prediction of progression after radical prostatectomy. Hum Pathol *27*, 683-687.
48. Winer, J., Jung, C.K., Shackel, I., and Williams, P.M. (1999). Development and validation of real-time quantitative reverse transcriptase-polymerase chain reaction for monitoring gene expression in cardiac myocytes in vitro. Analytical biochemistry *270*, 41-49.
49. Zaki, M.H., Nemeth, J.A., and Trikha, M. (2004). CNTO 328, a monoclonal antibody to IL-6, inhibits human tumor-induced cachexia in nude mice. Int J Cancer *111*, 592-595.